

# Open-Switch Fault Diagnosis System Based on One Current Sensing for a Matrix Converter Using Neural Network

Farzad Irajia<sup>a,\*</sup>, Alireza Nateghi<sup>b</sup>, Ebrahim Farjah<sup>a</sup>

<sup>a</sup>Shiraz University, Shiraz, Iran

<sup>b</sup>Shahid Beheshti University, Tehran, Iran

## Abstract

It is difficult to diagnose a three-phase matrix converter using a mathematical model, because a matrix converter consists of nine switches with various nonlinear factors. Since a neural network does not require any mathematical system model, it is a suitable technique for fault classification in matrix converters. In this manuscript, a fault diagnostic system for three-phase to three-phase matrix converters using a neural network is proposed to detect a fault and identify its location. The proposed diagnostic system can detect faults using just one phase current waveform which is very efficient in terms of cost of sensors and system complexity. This method was evaluated using simulation and experimental data sets in two scenarios. The results confirm that in different normal and abnormal situations the system achieves performance levels in excess of 98%.

**Keywords:** Fault Diagnosis, Matrix Converter, Neural Network

## Introduction

Compared to conventional AC/AC converters, the matrix converter (MC) is a power converter with numerous advantageous features, such as sinusoidal input or output currents, bi-directional power flow, four-quadrant operation, alterable power factor, no DC-link components and high power density [1, 2]. On account of these points of interest, MCs have been employed in various industrial fields, such as electric vehicles, aircraft, and other systems with exceptional demands for high temperature operation as well as space and weight savings [3]. Also, it is important for MCs to continue stable operation even after faults occur [4]. There are two types of faults in MC systems: open circuit and short circuit fault of power switches. For protection, a fast fuse is always placed in series with each switch. Therefore, short circuit faults will change into open circuit faults soon after the fault occurs. For greater reliability, fault diagnosis and fault tolerant capabilities are required for the MC [5–7]. In relation to this particular converter, some papers have been published on topics such as modulation strategies and topologies [8–13]. However, less effort has been devoted to fault diagnosis and fault tolerant strategies.

Fault tolerant configurations are the default technique to increase the reliability of power electronic systems [14]. All

the methods proposed in the literature in this regard can be categorized into two main solutions. In the first solution some extra components are utilized in the MC topology to reconfigure the faulty switches [15–18]. Cost, complexity and feasibility are the main drawbacks of the first solution. The second solution tries to modify the modulation strategy to control the remaining switches. For example, in [19] a fault tolerant space vector modulation (SVM) is proposed in which non-synthesizable vectors are replaced with synthesizable ones. All fault tolerant solutions are based on fault detection techniques. In other words, first a fault detection technique should identify the fault and the exact location of the faulty switch, and then the fault tolerant solutions would help with continuing the operation of the MC. In the literature, two major solutions have been proposed for detection and locating the open switch fault in MC. The first approach is signal processing based. In [20] discrete wavelet transform is employed to analyze the measured output current waveform to detect faults. However, the method is very complex and time consuming. The second approach is analytical based. Differences between the measured and reference line-to-line voltages can be used as the criterion for diagnosis purposes [15, 21–23]. This method will increase the system cost, since it requires voltage sensors on both sides of the MC. In [16] faulty switch identification is done using clamp and load currents, and a current sensor is required to measure the clamp current. In [24] a two-stage method is proposed in which the exact location of the fault is

\*Corresponding author

Email address: fziraji@gmail.com (Farzad Irajia)

determined by inspecting the load current. In [25] the load currents, duty-cycles of the switches, and the angles of the input and output voltages are used to help identify the fault. Artificial intelligence (AI)-based techniques can be utilized for fault diagnosis and condition monitoring. AI-based fault detection methods may have several benefits. For instance, there is no need to create a mathematical model of the system, just a data set of the system or even expert knowledge would suffice [26]. Various AI-based diagnosis systems have been proposed in the literature [27]. In [28] fast Fourier transform (FFT) and neural network (NN) are utilized to diagnose electrical machine faults. In [29] a fuzzy neural network is developed to diagnose faults of rotary machines. Some studies demonstrate that NNs can be used for system identification and fault detection [30].

The main contribution of this paper is to diagnose the fault location in a MC using current waveform of just one phase. Since there are nine switches in an MC, it is difficult to diagnose faults using mathematical models. Here, the NN method, which does not require a system model, has been employed to detect open switch fault. As will be discussed later in this paper, since the features extracted from the waveforms are very distinguishable, it is not necessary to use very accurate mathematical methods to be sure about the method output. The rest of the paper is organized in four sections. In the system description section, the overall system is described and the configuration of the diagnostic system is detailed. Then it goes on to discuss the feature extraction subsystem, which provides data for training NN. Experimental data set gathering for training of the NN is detailed. In the third section, a fault diagnostic system based on NN is described and various steps for training of NN are set out. Finally, in the results section the method is evaluated and the conclusion is presented.

## System Description

### Configuration of Fault Diagnostic System

The configuration of a fault diagnostic system is shown in Fig. 1. There are four major parts in the system, feature extraction, NN classification, fault diagnosis, and switching controller. The first three parts are the main focus of this paper. The feature extraction sub-system performs the transformation of output voltage and rated signals values, and the output of the sub-system is transferred to the NN classification. The NN are trained with both normal and abnormal data for the MC, and the output of the NN would be '0' and '1' as binary code. The binary code is decoded by a fault diagnosis sub-system to identify the fault and its location.

### Feature Extraction Sub-system

As mentioned earlier, the development of NN requires some data and the feature extraction sub-system generates the required data from the system waveforms. As shown in Fig. 1, the load of the MC is inductive and the switching

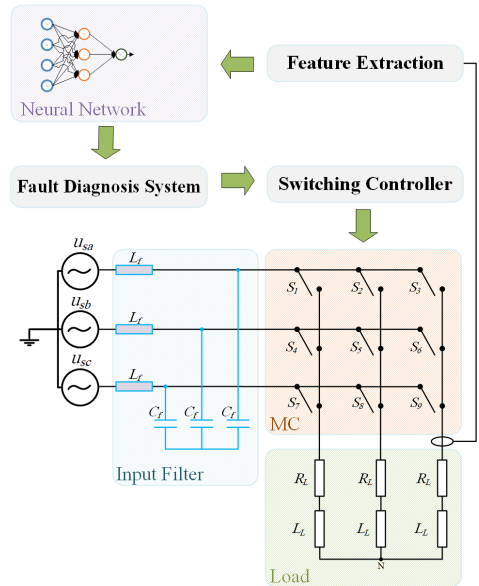


Figure 1: Configuration of the proposed fault diagnostic system

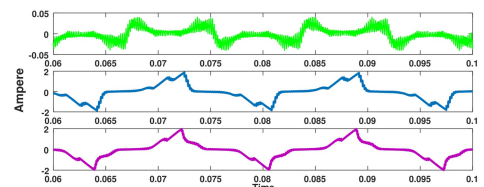


Figure 2: Simulation results of current waveform of phase "A" when the faulty switch is in phase "a" ( $S_1$  to  $S_3$  positions, respectively)

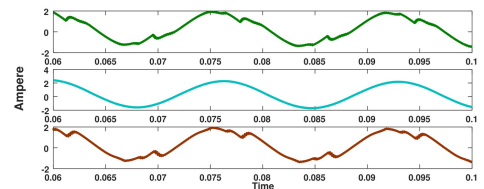


Figure 3: Simulation results of current waveform of phase "A" when the open switch is in phase "b" ( $S_4$  to  $S_6$  positions, respectively)

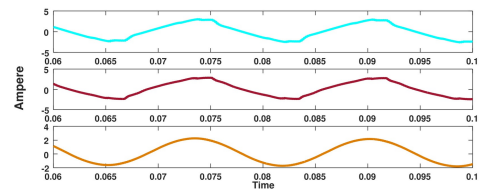


Figure 4: Simulation results of current waveform of phase "A" when the fault occurred in switches in phase "c" ( $S_7$  to  $S_9$  positions, respectively)

strategy is SVM. In Fig. 2, Fig. 3, and Fig. 4 current waveforms of phase A if the open switch fault occurs in phase a, b, and c are shown, respectively. In each figure, there are three sub-figures which present waveforms of different switches on each input phase. One can observe that all faults in different cases could be visually distinguishable, but the computation

unit cannot directly visualize as a human does. Therefore, a signal transformation technique is required. The feature extraction sub-system should provide the NN with sufficient important details of the pattern to make NN performance highly accurate. One efficient technique that can be implemented in digital signal processors (DSP) is FFT. The FFT technique is faster than other algorithms such as Hartley and wavelet, making it a more convenient method for an on-line fault diagnostic system. The FFT method is employed in this research for feature extraction. According to Fourier theory, a series of various sinusoidal frequencies can express any repetitive waveform.

Suppose  $i_s(t)$  is sampled as  $N$  discrete points using the sampling rate  $f_s$ , i.e. the truncation interval  $T = N/f_s$  (second). The sampling process is done by a DSP, and the continuous signal  $i_s(t)$  is converted to a discrete signal  $i_s[n]$ . This can be transformed by discrete Fourier transform (DFT) into the following equation.

$$I_s[k] = \frac{1}{N} \cdot \sum_{n=0}^{N-1} i_s[n] W_N^{kn} \quad (1)$$

where  $I_s[k]$  represents the discrete Fourier transform of  $i_s[n]$  at frequency  $f_k$ . i.e.  $f_k = k/T$ , and  $W_N = \exp(j2\pi/N)$ .

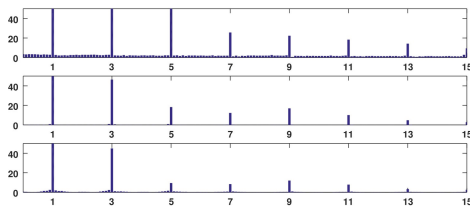


Figure 5: Transformed current waveforms of phase A, when faulty switch is in phase a ( $S_1$  to  $S_3$  positions, respectively)

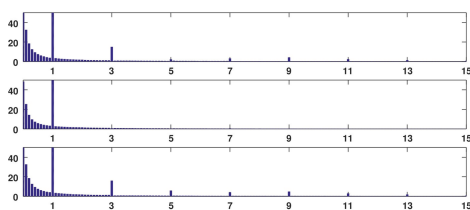


Figure 6: Transformed current waveforms of phase A, when faulty switch is in phase b ( $S_4$  to  $S_6$  positions, respectively)

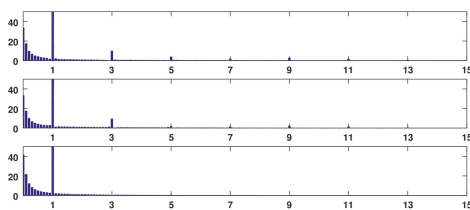


Figure 7: Transformed current waveforms of phase A, when opened switch is in phase c ( $S_7$  to  $S_9$  positions, respectively)

In Fig. 5, FFT has been employed to transform current waveforms if different switches in phase a are opened. A similar procedure is utilized for phases b and c, as illustrated in Fig. 6 and Fig. 7. It is clear that the transformed waveforms are different and more mathematically distinguishable.

Experimental setup

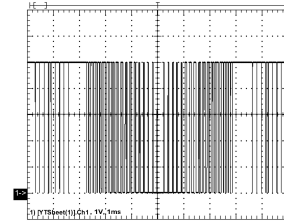


Figure 8: Gate switching signal for switch  $S_1$

A three-phase to three-phase matrix converter with SVM switching controller is implemented using 600 V, 80 A MOS-FETs. A PIC microcontroller is utilized to calculate and generate the gate signals. The SVM gate switching signals generated by the microcontroller, as shown in Fig. 8. The faults are produced manually by removing the switch in the desired location. All measured data are captured using a Tektronix oscilloscope, but the sampling rate is reduced to 500 kHz. Then the waveform’s features are extracted using FFT and, finally, the features are transferred to NN as the input.

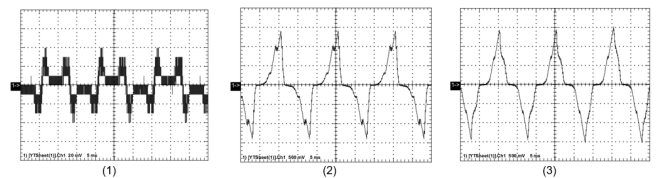


Figure 9: Experimental results of current waveform of phase “A”, when faulty switch is in  $S_1$  to  $S_3$  positions (phase “a”), respectively

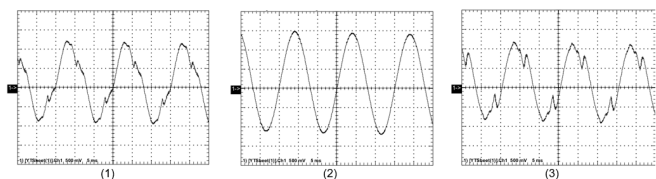


Figure 10: Experimental results of current waveform of phase “A”, when faulty switch is in  $S_4$  to  $S_6$  positions (phase “b”), respectively

Fig. 9 illustrates experimentally captured current waveforms of phase A when open switch fault occurs in different switches on phase a. Fig. 10 and Fig. 11 show the same waveform with different fault locations in phases b and c. As can be seen, the experimental results (Fig. 9 to Fig. 11) are similar to the results of the simulations (Fig. 2 to Fig. 4). It is obvious that the fault at different locations could be identified visually. If you can see the fault visually, the NN could perform the classification, too. As mentioned before, NN does

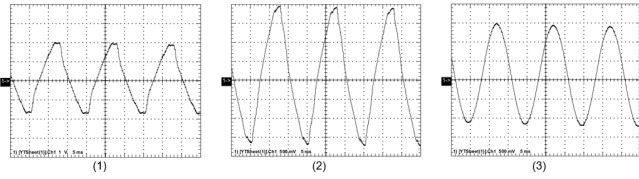


Figure 11: Experimental results of current waveform of phase “A”, when faulty switch is in  $S_7$  to  $S_9$  position (phase “c”), respectively

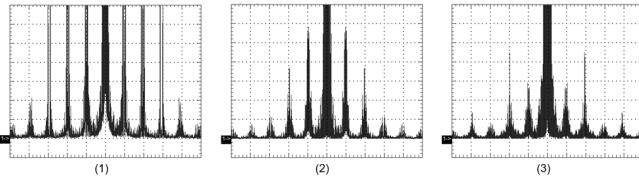


Figure 12: Transformed waveform of phase “A”, when faulty switch is in  $S_1$  to  $S_3$  positions (phase “a”), respectively

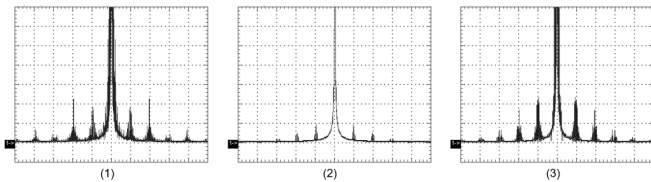


Figure 13: Transformed waveform of phase “A”, when faulty switch is in  $S_4$  to  $S_6$  position (phase “b”), respectively

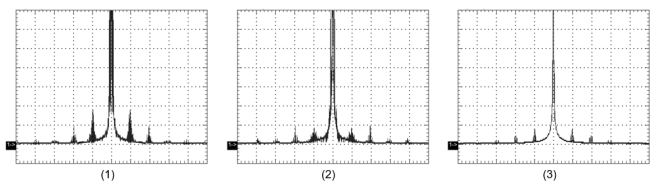


Figure 14: Transformed waveform of phase “A”, when faulty switch is in  $S_7$  to  $S_9$  position (phase “c”), respectively

not require a model of the system. Moreover, classification using the NN technique provides the system with other benefits. If one of the input neurons fails, the NN is still able to identify the fault using the other neurons. In contrast, a small change in the system or a sensor failure would cause the diagnosis system to fail. Here, the NN will be trained with data of different conditions, including different loads, therefore changes in the system will not cause any issue. Fig. 12 shows the transformed waveforms of the currents of phase A shown in Fig. 9. The transformed signals are similar to the results of the simulations, as was expected. Corresponding transformed waveforms for other phases are shown in Fig. 13 and Fig. 14.

In Fig. 5 and Fig. 12 the transformed signals of both experimental and simulation of phase a are illustrated, respectively. It is obvious that the results have nearly identical fault features, and the FFT technique efficiently identified the faulty and normal conditions. In each situation harmonic orders have different amplitudes. This confirms that the FFT is an efficient technique to classify normal and abnormal con-

ditions.

### Neural Network Fault Classification Approach

As mentioned earlier, all the features extracted can be classified by their effects on the waveform. Normally, systematic mathematical techniques are difficult to implement in real time control systems. Therefore, in a feedforward NN in which input/output mapping is permitted NN will be utilized. Also, the non-linear relationship between nodes can be considered. The real nature of the NN is to classify and generalize, this is why it can distinguish uncharacteristic conditions. Sensitivity and response time of the algorithm are suitable for on-line fault diagnosis. In the following different parts of the NN fault diagnosis methods are described.

### Design of Neural Network

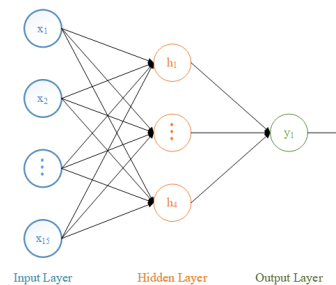


Figure 15: Architecture of the proposed fault diagnosis NN

Because of the input data characteristics, a multilayer feedforward NN is employed in this manuscript. The NN network has 15 input nodes representing a magnitude of each harmonic order. Also, the NN has one hidden layer with 4 nodes and one output node. It should be mentioned that the number of NN nodes varies for different applications. Therefore, the selection of dimensions of different layers in NN is based on the preferred level of accuracy. The *tansig* is used as the sigmoid activation function for hidden nodes and the output node. The proposed architecture of the fault diagnosis NN is shown in Fig. 15.

### Input/output Data

As mentioned earlier, the NN should be trained with a set of data. This data should contain normal and abnormal conditions. A forty set of normal data and a forty set of abnormal data for each switch is employed to train the NN, thus the size of the input matrix is 400 input data rows with 15 columns,  $[400 \times 15]$  and the size of the output target is  $[400 \times 1]$ . The output target relegates the number of faulty switches. Since the test data sets should consist of various operating regions, they are generated in different operating points. Data sets are sampled at 500 kHz and transformed by FFT to a set of 0 to 14 harmonic orders. To avoid saturation of sigmoidal units, the input training data sets are scaled by using the mean center and unit variance method.

Table 1: Confusion table for testing in the same operating points as the NN was trained

|                       |        | Actual Data |         |         |         |         |         |         |         |         |         |
|-----------------------|--------|-------------|---------|---------|---------|---------|---------|---------|---------|---------|---------|
|                       |        | Normal      | S1      | S2      | S3      | S4      | S5      | S6      | S7      | S9      | S9      |
| Classification Target | Normal | 99.70%      | 0.0280% | 0.0063% | 0.0540% | 0.0400% | 0.0089% | 0.0352% | 0.0322% | 0.0752% | 0.0195% |
|                       | S1     | 0.0678%     | 99.23%  | 0.1260% | 0.1005% | 0.1240% | 0.0300% | 0.1044% | 0.0153% | 0.1276% | 0.0744% |
|                       | S2     | 0.1768%     | 0.0352% | 99.02%  | 0.0024% | 0.1336% | 0.1847% | 0.0604% | 0.1540% | 0.1206% | 0.1122% |
|                       | S3     | 0.0229%     | 0.0033% | 0.0249% | 99.83%  | 0.0241% | 0.0014% | 0.0054% | 0.0501% | 0.0158% | 0.0220% |
|                       | S4     | 0.0803%     | 0.1122% | 0.0354% | 0.3279% | 98.91%  | 0.0108% | 0.0812% | 0.1816% | 0.2161% | 0.0447% |
|                       | S5     | 0.1517%     | 0.0948% | 0.0008% | 0.1412% | 0.1535% | 99.14%  | 0.0203% | 0.0915% | 0.0969% | 0.1093% |
|                       | S6     | 0.0117%     | 0.2003% | 0.0831% | 0.1357% | 0.2444% | 0.0042% | 98.97%  | 0.0429% | 0.0789% | 0.2287% |
|                       | S7     | 0.0547%     | 0.1741% | 0.0850% | 0.1046% | 0.0875% | 0.0326% | 0.1522% | 99.02%  | 0.0871% | 0.2022% |
|                       | S8     | 0.0616%     | 0.0378% | 0.0664% | 0.1072% | 0.0772% | 0.0575% | 0.0944% | 0.0012% | 99.40%  | 0.0967% |
|                       | S9     | 0.0404%     | 0.0133% | 0.0102% | 0.0894% | 0.0526% | 0.1135% | 0.0190% | 0.0128% | 0.0488% | 99.6%   |

Table 2: Confusion table for a different operating point

|                       |        | Actual Data |         |         |         |         |         |         |         |         |         |
|-----------------------|--------|-------------|---------|---------|---------|---------|---------|---------|---------|---------|---------|
|                       |        | Normal      | S1      | S2      | S3      | S4      | S5      | S6      | S7      | S8      | S9      |
| Classification Target | Normal | 98.52%      | 0.2514% | 0.2573% | 0.1799% | 0.0487% | 0.0444% | 0.2278% | 0.2366% | 0.2307% | 0.0032% |
|                       | S1     | 0.4632%     | 95.60%  | 0.7411% | 0.2972% | 0.0303% | 0.5579% | 0.5483% | 0.3445% | 0.6620% | 0.7554% |
|                       | S2     | 0.0482%     | 0.5649% | 96.53%  | 0.4404% | 0.7446% | 0.5019% | 0.2211% | 0.4447% | 0.3670% | 0.1372% |
|                       | S3     | 0.2549%     | 0.1092% | 0.3128% | 97.43%  | 0.3156% | 0.3261% | 0.2253% | 0.0306% | 0.5311% | 0.4646% |
|                       | S4     | 0.7753%     | 0.7738% | 0.7317% | 0.8400% | 93.07%  | 0.5413% | 0.4597% | 0.6996% | 1.1143% | 0.9943% |
|                       | S5     | 0.9227%     | 0.4337% | 0.6125% | 0.7909% | 0.7503% | 94.11%  | 0.7064% | 0.8777% | 0.7561% | 0.0395% |
|                       | S6     | 0.2311%     | 0.4512% | 0.1608% | 0.1399% | 0.4435% | 0.1712% | 97.80%  | 0.1267% | 0.3387% | 0.1370% |
|                       | S7     | 0.3918%     | 0.0197% | 0.2118% | 0.3818% | 0.3079% | 0.2849% | 0.1142% | 97.25%  | 0.3772% | 0.6607% |
|                       | S8     | 0.0988%     | 0.8599% | 0.9237% | 0.0342% | 1.2912% | 0.4714% | 0.3344% | 1.1648% | 94.64%  | 0.1817% |
|                       | S9     | 0.5754%     | 0.1009% | 0.5943% | 0.1716% | 0.4781% | 0.4097% | 0.3698% | 0.3634% | 0.8668% | 96.07%  |

### Neural Network Training

The Levenberg Marquardt algorithm is used to train the NN; it requires more memory but less time. This method has intrinsic regularization properties, which adds constraints to make the results more consistent. The NN training is accomplished when generalization stops improving, as indicated by variations in the mean square error of the validation samples. For calculation of the sum of square error (SSE), misclassification and input data error rate are chosen. Using the following equation SSE can be calculated as 0.05.

$$SSE = \sqrt{\frac{1}{N} \cdot \sum_{i=1}^N \sum_{j=1}^L (y_{ij} - d_{ij})^2} \quad (2)$$

where  $y_{ij}$  is output of the NN,  $d_{ij}$  is output of training data,  $N$  is number of training data, and  $L$  is number of units in the output layer.

### Fault Classification Results

To evaluate the proposed method, two different scenarios are considered. In the first scenario, the method is evaluated using data sets gathered from the system in the same operating points where the NN was trained. In Table 1 the testing data along with the tested results are tabulated. The error

between the actual value and the target data should be less than the SSE goal. Therefore, according to Table 1 it is confirmed that the training process is complete. Performance of the NN classification is evidently more than 98.9%. Thus, when the operating point is same as in the trained data sets, the NN could properly identify the faults in different switches.

In the second scenario, a new operating point is considered so as to test the trained NN. This new operating point is established by changing the load values in the training data load range. Ideally, the diagnostic system should have good performance in terms of identifying the faults for a wide range of the operating point. The results are tabulated in Table 2. In this scenario, the classification performance between normal and abnormal is more than 98%, which is very impressive. Also, the classification performance in different fault locations is about 93%. The NN classification performance for fault identification is very good. However, the NN could be trained using a larger data set to make the fault classifying results more accurate. While the results are relatively accurate, better results might be achieved by employing other feature extraction methods.

## Conclusion

This paper proposes a fault diagnostic system for matrix converters using a neural network. A feature extraction subsystem based on the FFT technique is utilized to transform output waveforms. The transformed waveforms are used as NN inputs. The FFT method has advantages in the form of fast computation and ready implementation in most digital signal processing microchips and microcontrollers. Finding an efficient method for the feature extraction subsystem is a challenge. The proposed diagnosis system is adept at identifying a fault and its location. The proposed method is evaluated using simulation and experimental data in two different scenarios. The classification performance is in excess of 98%. The evaluations confirm the accuracy of the proposed method in detecting and locating the faulty switch.

## References

- [1] Bin Wu and Mehdi Narimani. *High-power converters and AC drives*, volume 59. John Wiley & Sons, 2017.
- [2] Sergio Vazquez, Jose Rodriguez, Marco Rivera, Leopoldo G Franquelo, and Margarita Norambuena. Model predictive control for power converters and drives: Advances and trends. *IEEE Transactions on Industrial Electronics*, 64(2):935–947, 2016.
- [3] Eiji Yamamoto, Hidenori Hara, Takahiro Uchino, Masahiro Kawaji, Tsuneo Joe Kume, Jun Koo Kang, and Hans-Peter Krug. Development of MCs and its Applications in Industry [Industry Forum]. *IEEE Industrial Electronics Magazine*, 5(1):4–12, mar 2011.
- [4] M. Aten, G. Towers, C. Whitley, P. Wheeler, J. Clare, and K. Bradley. Reliability comparison of matrix and other converter topologies. *IEEE Transactions on Aerospace and Electronic Systems*, 42(3):867–875, jul 2006.
- [5] Ui-Min Choi, Frede Blaabjerg, and Kyo-Beum Lee. Study and Handling Methods of Power IGBT Module Failures in Power Electronic Converter Systems. *IEEE Transactions on Power Electronics*, 30(5):2517–2533, may 2015.
- [6] Hyunseok Oh, Bongtae Han, Patrick McCluskey, Changwoon Han, and Byeng D. Youn. Physics-of-Failure Condition Monitoring, and Prognostics of Insulated Gate Bipolar Transistor Modules: A Review. *IEEE Transactions on Power Electronics*, 30(5):2413–2426, may 2015.
- [7] Wenping Zhang, Dehong Xu, Prasad N. Enjeti, Haijin Li, Joshua T. Hawke, and Harish S. Krishnamoorthy. Survey on Fault-Tolerant Techniques for Power Electronic Converters. *IEEE Transactions on Power Electronics*, 29(12):6319–6331, dec 2014.
- [8] Yao Sun, Wenjing Xiong, Mei Su, Xing Li, Hanbing Dan, and Jian Yang. Topology and modulation for a new multilevel diode-clamped matrix converter. *IEEE Transactions on Power Electronics*, 29(12):6352–6360, 2014.
- [9] Johann W Kolar, Frank Schafmeister, Simon D Round, and Hans Ertl. Novel three-phase AC–AC sparse matrix converters. *IEEE transactions on power electronics*, 22(5):1649–1661, 2007.
- [10] L. Huber and D. Borojovic. Space vector modulated three-phase to three-phase matrix converter with input power factor correction. *IEEE Transactions on Industry Applications*, 31(6):1234–1246, 1995.
- [11] D. Casadei, G. Serra, A. Tani, and L. Zarri. Matrix converter modulation strategies: a new general approach based on space-vector representation of the switch state. *IEEE Transactions on Industrial Electronics*, 49(2):370–381, apr 2002.
- [12] Yao Sun, Wenjing Xiong, Mei Su, Xing Li, Hanbing Dan, and Jian Yang. Carrier-Based Modulation Strategies for Multimodular Matrix Converters. *IEEE Transactions on Industrial Electronics*, 63(3):1350–1361, mar 2016.
- [13] Yao Sun, Wenjing Xiong, Mei Su, Hanbing Dan, Xing Li, and Jian Yang. Modulation Strategies Based on Mathematical Construction Method for Multimodular Matrix Converter. *IEEE Transactions on Power Electronics*, 31(8):5423–5434, aug 2016.
- [14] Huai Wang, Marco Liserre, Frede Blaabjerg, Peter de Place Rimmen, John B. Jacobsen, Thorkild Kvisgaard, and Jorn Landkildehus. Transitioning to Physics-of-Failure as a Reliability Driver in Power Electronics. *IEEE Journal of Emerging and Selected Topics in Power Electronics*, 2(1):97–114, mar 2014.
- [15] Sangshin Kwak. Fault-Tolerant Structure and Modulation Strategies With Fault Detection Method for Matrix Converters. *IEEE Transactions on Power Electronics*, 25(5):1201–1210, may 2010.
- [16] Sudarat Khwan-on, Liliana de Lillo, Lee Empringham, and Pat Wheeler. Fault-Tolerant Matrix Converter Motor Drives With Fault Detection of Open Switch Faults. *IEEE Transactions on Industrial Electronics*, 59(1):257–268, jan 2012.
- [17] Sangshin Kwak and Hamid A. Toliyat. Fault-Tolerant Topologies and Switching Function Algorithms for Three-Phase Matrix Converter based AC Motor Drives Against Open and Short Phase Failures. In *2007 IEEE International Electric Machines & Drives Conference*. IEEE, may 2007.
- [18] Sangshin Kwak. Four-Leg-Based Fault-Tolerant Matrix Converter Schemes Based on Switching Function and Space Vector Methods. *IEEE Transactions on Industrial Electronics*, 59(1):235–243, jan 2012.
- [19] Edorta Ibarra, Jon Andreu, Inigo Kortabarria, Enekoitz Ormaetxea, and Eider Robles. A fault tolerant space vector modulation strategy for matrix converters. In *2009 35th Annual Conference of IEEE Industrial Electronics*. IEEE, nov 2009.
- [20] Panagiotis G. Potamianos, Epaminondas D. Mitronikas, and Athanasios N. Safacas. Open-Circuit Fault Diagnosis for Matrix Converter Drives and Remedial Operation Using Carrier-Based Modulation Methods. *IEEE Transactions on Industrial Electronics*, 61(1):531–545, jan 2014.
- [21] Steven X Ding. *Model-based fault diagnosis techniques: design schemes, algorithms, and tools*. Springer Science & Business Media, 2008.
- [22] S.M.A. Cruz, M. Ferreira, and A.J.M. Cardoso. Output error voltages - a first method to detect and locate faults in matrix converters. In *2008 34th Annual Conference of IEEE Industrial Electronics*. IEEE, nov 2008.
- [23] Sérgio M. A. Cruz, Marco Ferreira, André M. S. Mendes, and António J. Marques Cardoso. Analysis and Diagnosis of Open-Circuit Faults in Matrix Converters. *IEEE Transactions on Industrial Electronics*, 58(5):1648–1661, may 2011.
- [24] Khiem Nguyen-Duy, Tian-Hua Liu, Der-Fa Chen, and John Y. Hung. Improvement of Matrix Converter Drive Reliability by Online Fault Detection and a Fault-Tolerant Switching Strategy. *IEEE Transactions on Industrial Electronics*, 59(1):244–256, jan 2012.
- [25] Sérgio M. A. Cruz, André M. S. Mendes, and António J. Marques Cardoso. A New Fault Diagnosis Method and a Fault-Tolerant Switching Strategy for Matrix Converters Operating With Optimum Alesina-Venturini Modulation. *IEEE Transactions on Industrial Electronics*, 59(1):269–280, jan 2012.
- [26] Peter Vas. *Artificial-intelligence-based electrical machines and drives: application of fuzzy, neural, fuzzy-neural, and genetic-algorithm-based techniques*, volume 45. Oxford university press, 1999.
- [27] F. Fiappetti and P. Vas. Recent developments of induction motor drives fault diagnosis using AI techniques. In *IECON 98. Proceedings of the 24th Annual Conference of the IEEE Industrial Electronics Society (Cat. No.98CH36200)*. IEEE.
- [28] S. Hayashi, T. Asakura, and Sheng Zhang. Study of machine fault diagnosis system using neural networks. In *Proceedings of the 2002 International Joint Conference on Neural Networks. IJCNN02 (Cat. No.02CH37290)*. IEEE.
- [29] Sheng ZHANG, Toshiyuki ASAKURA, Xiaoli XU, and Baojie XU. Fault Diagnosis System for Rotary Machine Based on Fuzzy Neural Networks. *JSME International Journal Series C*, 46(3):1035–1041, 2003.
- [30] A. Bernieri, M. DApuzzo, L. Sansone, and M. Savastano. A neural network approach for identification and fault diagnosis on dynamic systems. *IEEE Transactions on Instrumentation and Measurement*, 43(6):867–873, 1994.